Published in final edited form as:
Nat Genet. 2009 September ; 41(9): 1037–1042. doi:10.1038/ng.422.

FOXC1 is required for normal cerebellar development and is a major contributor to chromosome 6p25.3 Dandy-Walker malformation

Kimberly A Aldinger[1], **Ordan J Lehmann**[2], **Louanne Hudgins**[3], **Victor V Chizhikov**[4], **Alexander G Bassuk**[5], **Lesley C Ades**[6,7], **Ian D Krantz**[8], **William B Dobyns**[4,9], and **Kathleen J Millen**[1,4,9]

[1]Committee on Neurobiology, University of Chicago, Chicago, Illinois, USA.

[2]Departments of Ophthalmology and Medical Genetics, University of Alberta, Edmonton, Canada.

[3]Division of Medical Genetics, Department of Pediatrics, Stanford University, Stanford, California, USA.

[4]Department of Human Genetics, University of Chicago, Chicago, Illinois, USA.

[5]Department of Pediatrics, Division of Neurology and the Interdisciplinary Graduate Program in Genetics, University of Iowa, Iowa City, Iowa, USA.

[6]Department of Clinical Genetics, The Children's Hospital at Westmead, Sydney, New South Wales, Australia.

[7]Discipline of Paediatrics and Child Health, University of Sydney, Sydney, New South Wales, Australia.

[8]Division of Human Genetics, The Children's Hospital of Philadelphia, Philadelphia, Pennsylvania, USA.

[9]Department of Neurology, University of Chicago, Chicago, Illinois, USA.

Abstract

Dandy-Walker malformation (DWM), the most common human cerebellar malformation, has only one characterized associated locus[1,2]. Here we characterize a second DWM-linked locus on 6p25.3, showing that deletions or duplications encompassing *FOXC1* are associated with cerebellar and posterior fossa malformations including cerebellar vermis hypoplasia (CVH), mega-cisterna magna (MCM) and DWM. *Foxc1*-null mice have embryonic abnormalities of the rhombic lip due to loss of mesenchyme-secreted signaling molecules with subsequent loss of Atoh1 expression in vermis. *Foxc1* homozygous hypomorphs have CVH with medial fusion and foliation defects. Human

Correspondence should be addressed to K.J.M. (kmillen@genetics.bsd.uchicago.edu).

AUTHOR CONTRIBUTIONS

K.A.A. contributed to study design and performed most human and mouse studies and manuscript writing. O.J.L. provided brain scans for multiple individuals and contributed to data analysis and manuscript writing. V.V.C. contributed to mouse immunohistochemical studies. L.H., A.G.B. and L.C.A. provided key phenotype data on one or more individuals. I.D.K. provided much of the initial ideas and data used to start this project, as well as new phenotype data on one subject. W.B.D. contributed to the initial design of the study, patient ascertainment, clinical evaluation including interpretation of all brain scans, delineation of the phenotype and manuscript writing. K.J.M. designed the study, supervised the mouse studies and contributed to manuscript writing.

Note: Supplementary information is available on the Nature Genetics website.

FOXC1 heterozygous mutations are known to affect eye development, causing a spectrum of glaucoma-associated anomalies (Axenfeld-Rieger syndrome, ARS; MIM no. 601631). We report the first brain imaging data from humans with *FOXC1* mutations and show that these individuals also have CVH. We conclude that alteration of *FOXC1* function alone causes CVH and contributes to MCM and DWM. Our results highlight a previously unrecognized role for mesenchyme-neuroepithelium interactions in the mid-hindbrain during early embryogenesis.

Malformations of the cerebellum are common, heterogeneous human birth defects with chromosomal, single-gene and complex inheritance[1–3]. CVH, MCM and DWM are generally classified as separate disorders, but they overlap in appearance, and it remains unclear whether they represent distinct entities or share a common pathogenesis[1,3,4]. We found reports supporting four classic DWM-associated loci, including chromosome 3q24 and 6p25.3, with brain imaging documentation (Supplementary Table 1). We previously identified heterozygous deletion of *ZIC1* and *ZIC4* on 3q24 as the first molecularly defined cause of classic DWM (MIM no. 220200)2 and mapped a second locus to a 1.8-Mb critical region on 6p25.3 (refs. 5,6).

To define this second locus, we obtained brain imaging studies and mapped the breakpoint in 12 individuals with deletion and 6 with duplication of 6p25.3, all ascertained because of multiple congenital anomalies, especially eye malformations consistent with ARS. Anterior chamber dysgenesis was observed in 17/18 affected individuals5,7–9, but too few details were available to compare severity (data not shown). We have even fewer data regarding the retina, although two of the affected individuals had microphthalmia with posterior colobomas. Further, most were examined at a single time point, whereas the ocular abnormalities associated with ARS are known to vary with time (for example, progressive iris alterations or development of glaucoma between 0 and 40 years). Both of these factors limit genotype-phenotype correlation. Brain imaging studies were previously reported for only 5/18 of these individuals5,8. Data illustrated in the first two figures include copy number variants (CNVs), known genes in the region (Fig. 1), brain phenotype details (Table 1) and imaging studies (Fig. 2). One affected individual reported to harbor a telomeric deletion[8] proved upon after oligonucleotide array analysis to have a 450-kb segmental deletion (Supplementary Fig. 1). Among the 12 individuals with deletions, 4 were *de novo*, 3 derived from parental translocations, 2 familial and 3 of unknown origin (Table 1). The duplications were inherited from a common founder[9].

In general, the brain imaging studies show four overlapping malformation groups: in order of severity, classic DWM, mild DWM, MCM and isolated CVH. The six affected individuals with large deletions involving at least seven genes (*IRF4* to *GMDS*) have the most severe brain phenotypes, with classic DWM in four and mild DWM in another. The sixth has normal vermis size but other subtle defects (**Supplementary Note**). The four individuals with smaller deletions involving the forkhead transcription factor *FOXC1* and all or part of *GMDS* (GDP-mannose-4,6-dehydratase) have less severe phenotypes, with mild DWM in the two individuals with 450- and 870-kb deletions and even less severe MCM or CVH in the sibs with the 30-kb deletion.

Our combined genotype and phenotype data show consistently more severe phenotypes among individuals with large compared to small deletions, which implicates contributions from more than one causative gene in the region. Further, all 12 affected individuals had deletions of *FOXC1* plus at least two exons of *GMDS*, implicating one or both of these genes as having a previously unrecognized role in cerebellar development. This conclusion is further supported by the results of brain imaging in six affected individuals with small (~492-kb) duplications (*FOXF2-FOXC1-GMDS*), who also showed MCM or CVH, much like the individuals with the smallest 6p25.3 deletions.

We concurrently evaluated the developmental expression profiles of the eight known genes in the 1.8-Mb initial DWM critical region in mice and examined cerebellar morphology in available mutants (Supplementary Table 2). Neither *Gmds* nor *Foxc1* are expressed in the developing brain, although *Foxc1* is expressed in the mesenchyme covering the developing cerebellum (Fig. 3a,b and data not shown). We found that *Foxc1*-mutant mice have a marked cerebellar malformation (Fig. 3–Fig. 5), supporting our hypothesis that *FOXC1* is involved in human 6p25.3 associated DWM.

The *Foxc1* gene is widely expressed in mesenchyme and its protein product participates in a broad range of developmental processes including somatic, cardiovascular, kidney, eye, skull and cortical development, but no cerebellar phenotypes have been associated with mutations in this gene[10–15]. It is never expressed in the cerebellum itself, but it is expressed in the adjacent posterior fossa mesenchyme starting from embryonic day (E) 11.5 (data not shown). The earliest defect we observed in *Foxc1*-null (*Foxc1* $^{-/-}$) mouse embryos was an enlarged fourth ventricle roof plate at E12.5 (Fig. 3c – e). By E14.5, the cerebellar rhombic lip induced by the rhombomere 1 roof plate was disorganized (Fig. 3g), with the presumptive external granule layer (EGL) forming a clump rather than a thin layer covering the nascent cerebellum. By E17.5, the *Foxc1* $^{-/-}$ cerebellum was small, lacked posterior foliation and showed deficient midline fusion (Fig. 3i). Later stages could not be examined due to perinatal lethality.

The roof plate and rhombic lip are transient embryonic structures required for proper cerebellar development[16–18]. Results from molecular analyses of early roof plate and rhombic lip specification, induction (Supplementary Fig. 2 and 3) and anlage proliferation (data not shown) in *Foxc1* $^{-/-}$ embryos were normal. We next examined markers of differentiating cell types that arise in successive waves from the rhombic lip[1,19]. At E12.5, ectopic Ttr^{+} choroid plexus epithelium spanned the midline roof plate in *Foxc1* $^{-/-}$ embryos (Fig. 4a), correlating with the roof plate morphologic change. At E14.5, Tbr1^{+} deep cerebellar nuclei cells were normal (Supplementary Fig. 4), an expected finding as these cells are generated and migrate from the rhombic lip before the E11.5 onset of posterior fossa *Foxc1* expression. Expression of *Atoh1* (previously *Math1*), a marker of rhombic lip and EGL cells, was normal at E12.5, but medial expression was lost by E14.5 (Fig. 4b). The Atoh1^{-} cells in the medial EGL domain were Zic1^{+} and Pax6^{+}, and they continued to proliferate, confirming their EGL identity (Supplementary Fig. 4 and data not shown). The failure of EGL migration was not accounted for by substrate loss, as the basement membrane at the pial surface of the cerebellum was intact at E14.5. Eomes^{+} (previously Tbr2^{+}) unipolar brush cells, the last derivative to leave the rhombic lip, were present in *Foxc1* $^{-/-}$ embryos at E18.5 but did not migrate away from the rhombic lip (Fig. 4c). Many of these phenotypes can be attributed to loss of medial Atoh1 expression[20]. Together, our data demonstrate that *Foxc1* is required to direct the normal differentiation and migration of roof plate and rhombic lip derivatives but is not required for the progression of cell fate specification in the rhombic lip.

Foxc1 expression in mesenchyme influences the proliferation and differentiation of eye and endothelial development by regulating secreted signaling molecules that include Bmp2, Bmp4, Cxcl12 and Tgfb1 (refs. 21–23). We examined expression of these signaling molecules in E12.5 *Foxc1* $^{-/-}$ hindbrain (posterior fossa) to test whether the same molecules direct cerebellar development. All four were significantly reduced in posterior fossa mesenchyme (Fig. 4d and Supplementary Fig. 5). These data provide a possible mechanism by which nonautonomous loss of Foxc1 leads to a severe cerebellar phenotype, as Bmp2, Bmp4 and Cxcl12 are essential for normal EGL development at later postnatal stages[18,24] and Bmp signaling is known to be critical for Atoh1 expression[16,18,25,26]. It remains possible that additional signaling pathways influence Atoh1 expression. Because our data show that Foxc1-dependent signaling from head mesenchyme also regulates roof plate development, it is possible that some defects in granule cell migration may be mediated by abnormal roof plate signaling.

Although complete loss of *Foxc1* in mice causes perinatal lethality and a severe cerebellar phenotype, homozygous *Foxc1* hypomorphs (*Foxc1* $^{hith/hith}$), carrying a protein-destabilizing point mutation, survive to adulthood[15]. We observed that *Foxc1* $^{hith/hith}$ mice were ataxic and had CVH combined with defects in midline vermis fusion and folial patterning (Fig. 5). These changes resemble the cerebellar phenotypes seen in individuals with 6p25.3-associated DWM, prompting us to ask whether intragenic mutations of *FOXC1* in humans also result in a cerebellar phenotype. We therefore assessed brain imaging studies from three affected individuals, originally ascertained because of anterior eye defects, who harbored heterozygous *FOXC1* point mutations in the coding region (resulting in the amino acid substitutions S82T27,28 and S131L29). Both mutations were previously shown to disrupt DNA binding *in vitro* [30]. All three of these individuals have mild CVH with normal vermis position and posterior fossa size (Fig. 1 and Fig. 2m–o), proving that partial loss of *FOXC1* alone results in a cerebellar malformation in humans.

Our mouse data provide the first evidence that altered gene expression in mesenchyme can result in cerebellar malformation. Because cranial mesenchyme differentiates into skull and meninges surrounding the brain, we also examined the brain imaging studies from our cohort of subjects with 6p25.3 mutations for developmental defects of these structures. We found meningeal defects leading to abnormal positioning of cerebral gyri in 6/17 (Supplementary Fig. 6 and **Supplementary Note**) and enlarged posterior fossae (MCM plus DWM) in 12/21 affected individuals. These findings led us to hypothesize that the enlarged posterior fossa characteristic of MCM and DWM, and the meningeal deficiency, result from defective mesenchymal signaling rather than from increased intracranial pressure or other previously proposed mechanisms[3,4].

In examining our entire cohort of affected individuals, including those with intragenic *FOXC1* mutations, we found complete penetrance and variable expressivity, although with a consistent genotype-phenotype correlation. The cerebellar malformations were most severe with large 6p25.3 deletions, intermediate with small deletions or duplications, and least severe with intragenic *FOXC1* point mutations (Fig. 1 and Fig. 2). This suggests that loss (or gain) of *FOXC1* alone is sufficient to cause isolated CVH and contribute to the more severe MCM and DWM phenotypes, whereas loss (or gain) of additional genes increases the likelihood of a more severe phenotype. The phenotypes of intermediate severity found with small deletions or duplications suggest that the nearby genes *FOXF2* or *GMDS* contribute to the more severe phenotype, but other genes may also be involved, given the consistently greater severity that accompanies the very large deletions. We examined the expression of all eight genes within the 6p25.3 DWM locus in control human lymphoblastoid cell lines (LBLs) and found that most genes were expressed at very low or undetectable levels (**Supplementary Fig. 7**). Therefore, evaluation of gene expression in LBLs derived from individuals with 6p25.3 CNVs is unlikely to aid our understanding of which additional 6p25.3 genes contribute to the severity of cerebellar phenotypes.

FOX genes exist mostly in clusters throughout the genome and often act synergistically[31]. Three *FOX* genes (*FOXQ1*, *FOXF2* and *FOXC1*) occur in tandem within 6p25.3. In mice, *Foxf2* briefly shares the *Foxc1* hindbrain mesenchyme expression domain[32], and *Foxc1* and *Foxq1* are each required for proper endothelial development[13,23,33,34]. No brain phenotype has been reported in *Foxq1*$^{-/-}$ or *Foxf2*$^{-/-}$ mice, and our examination did not reveal morphological changes in the cerebellum of either mutant (Supplementary Table 2 and data not shown). However, the regulation of cerebellar development via genetic interaction among *Foxq1*, *Foxf2* and *Foxc1* has not been evaluated and remains a plausible cause for the severe cerebellar phenotype observed among humans with large 6p25.3 deletions.

Considered together, our data demonstrate that specific loss of *FOXC1* and general defects in mesenchymal signaling may result in cerebellar malformations and that the clinical diagnoses of isolated CVH, MCM and DWM belong to a single spectrum with shared etiology in some affected individuals. Our observations have several important implications beyond the developmental biology of these phenotypes. First, the clinical difficulty in distinguishing between isolated CVH, MCM and DWM becomes understandable, and our results should thus lead to more flexible diagnostic criteria. Second, classic DWM is frequently associated with hydrocephalus caused by an unknown mechanism. Our data demonstrate a consistent and unequivocal expansion of the choroid plexus epithelium in *Foxc1*$^{-/-}$ mice. We propose that increased cerebrospinal fluid production by an enlarged choroid plexus contributes to hydrocephalus in humans, but this hypothesis requires further analysis in mouse models. Finally, mutations of other genes such as *OPHN1* and *CASK* are associated with CVH or diffuse cerebellar hypoplasia but not with MCM or DWM[35,36]. Our current working hypothesis is that genes with primary cerebellar expression will be associated with CVH or diffuse cerebellar hypoplasia, whereas genes with posterior fossa mesenchymal expression will be associated with the complete CVH-MCM-DWM spectrum of malformations.

METHODS

Methods and any associated references are available in the online version of the paper at http://www.nature.com/naturegenetics/.

Supplementary Material

Refer to Web version on PubMed Central for supplementary material.

Acknowledgments

We thank the affected individuals and their families for their participation; C. Beaulieu for assistance with MRI; T. Kume for providing *Foxc1* $^{+/-}$ mice; S. Pleasure and A. Peterson for *Foxc1* $^{+/hith}$ mice; H. Sing, H. Hang, R. Arkell, N. Miura, J. Belmont, Q. Ma, B. Hogan, W. Duan, J. Johnson, M.E. Hatten, R. Miller, E. Grove, M. German, T. Jessell and R. Hevner for providing mutant brains, *in situ* probes or antibodies; and M. Walter for helpful discussions. This work was supported by the following awards: an Autism Speaks predoctoral fellowship to K.A.A., Alberta Heritage for Medical Research and Canadian Institute for Health Research grants to O.J.L., US National Institutes of Health grants KO8-NS48174-01A to A.G.B., R01-NS050375 to W.B.D. and R01-NS050386 to K.J.M., and March of Dimes Birth Defects Foundation award 6-FYO7-334 to K.J.M.

References

1. Millen KJ, Gleeson JG. Cerebellar development and disease. Curr. Opin. Neurobiol 2008;18:12–19. [PubMed: 18513948]
2. Grinberg I, et al. Heterozygous deletion of the linked genes *ZIC1* and *ZIC4* is involved in Dandy-Walker malformation. Nat. Genet 2004;36:1053–1055. [PubMed: 15338008]
3. Parisi MA, Dobyns WB. Human malformations of the midbrain and hindbrain: review and proposed classification scheme. Mol. Genet. Metab 2003;80:36–53. [PubMed: 14567956]
4. Patel S, Barkovich AJ. Analysis and classification of cerebellar malformations. AJNR Am. J. Neuroradiol 2002;23:1074–1087. [PubMed: 12169461]
5. DeScipio C, et al. Subtelomeric deletions of chromosome 6p: molecular and cytogenetic characterization of three new cases with phenotypic overlap with RitscherSchinzel (3C) syndrome. Am. J. Med. Genet. A 2005;134:3–11. [PubMed: 15704124]
6. DeScipio C, et al. Fine-mapping subtelomeric deletions and duplications by comparative genomic hybridization in 42 individuals. Am. J. Med. Genet. A 2008;146A:730–739. [PubMed: 18257100]
7. Lin RJ, et al. Terminal deletion of 6p results in a recognizable phenotype. Am. J. Med. Genet. A 2005;136:162–168. [PubMed: 15940702]

8. Maclean K, et al. Axenfeld-Rieger malformation and distinctive facial features: clues to a recognizable 6p25 microdeletion syndrome. Am. J. Med. Genet. A 2005;132:381–385. [PubMed: 15654696]
9. Chanda B, et al. A novel mechanistic spectrum underlies glaucoma-associated chromosome 6p25 copy number variation. Hum. Mol. Genet 2008;17:3446–3458. [PubMed: 18694899]
10. Kume T, et al. The forkhead/winged helix gene Mf1 is disrupted in the pleiotropic mouse mutation congenital hydrocephalus. Cell 1998;93:985–996. [PubMed: 9635428]
11. Kume T, Deng K, Hogan BL. Murine forkhead/winged helix genes *Foxc1* (*Mf1*) and *Foxc2* (*Mfh1*) are required for the early organogenesis of the kidney and urinary tract. Development 2000;127:1387–1395. [PubMed: 10704385]
12. Kume T, Jiang H, Topczewska JM, Hogan BL. The murine winged helix transcription factors, Foxc1 and Foxc2, are both required for cardiovascular development and somitogenesis. Genes Dev 2001;15:2470–2482. [PubMed: 11562355]
13. Seo S, et al. The forkhead transcription factors, Foxc1 and Foxc2, are required for arterial specification and lymphatic sprouting during vascular development. Dev. Biol 2006;294:458–470. [PubMed: 16678147]
14. Wilm B, James RG, Schultheiss TM, Hogan BL. The forkhead genes, Foxc1 and Foxc2, regulate paraxial versus intermediate mesoderm cell fate. Dev. Biol 2004;271:176–189. [PubMed: 15196959]
15. Zarbalis K, et al. Cortical dysplasia and skull defects in mice with a *Foxc1* allele reveal the role of meningeal differentiation in regulating cortical development. Proc. Natl. Acad. Sci. USA 2007;104:14002–14007. [PubMed: 17715063]
16. Chizhikov VV, et al. The roof plate regulates cerebellar cell-type specification and proliferation. Development 2006;133:2793–2804. [PubMed: 16790481]
17. Wingate R. Math-Map(ic)s. Neuron 2005;48:1–4. [PubMed: 16202701]
18. Alder J, Lee KJ, Jessell TM, Hatten ME. Generation of cerebellar granule neurons *in vivo* by transplantation of BMP-treated neural progenitor cells. Nat. Neurosci 1999;2:535–540. [PubMed: 10448218]
19. Hevner RF, Hodge RD, Daza RA, Englund C. Transcription factors in glutamatergic neurogenesis: conserved programs in neocortex, cerebellum, and adult hippocampus. Neurosci. Res 2006;55:223–233. [PubMed: 16621079]
20. Ben-Arie N, et al. Atoh1 is essential for genesis of cerebellar granule neurons. Nature 1997;390:169–172. [PubMed: 9367153]
21. Rice R, Rice DP, Thesleff I. Foxc1 integrates Fgf and Bmp signalling independently of twist or noggin during calvarial bone development. Dev. Dyn 2005;233:847–852. [PubMed: 15906377]
22. Sommer P, Napier HR, Hogan BL, Kidson SH. Identification of Tgf beta1i4 as a downstream target of Foxc1. Dev. Growth Differ 2006;48:297–308. [PubMed: 16759280]
23. Hayashi H, Kume T. Forkhead transcription factors regulate expression of the chemokine receptor CXCR4 in endothelial cells and CXCL12-induced cell migration. Biochem. Biophys. Res. Commun 2008;367:584–589. [PubMed: 18187037]
24. Ma Q, et al. Impaired B-lymphopoiesis, myelopoiesis, and derailed cerebellar neuron migration in CXCR4- and SDF-1-deficient mice. Proc. Natl. Acad. Sci. USA 1998;95:9448–9453. [PubMed: 9689100]
25. Krizhanovsky V, Ben-Arie N. A novel role for the choroid plexus in BMP-mediated inhibition of differentiation of cerebellar neural progenitors. Mech. Dev 2006;123:67–75. [PubMed: 16325379]
26. Qin L, Wine-Lee L, Ahn KJ, Crenshaw EB III. Genetic analyses demonstrate that bone morphogenetic protein signaling is required for embryonic cerebellar development. J. Neurosci 2006;26:1896–1905. [PubMed: 16481421]
27. Mears AJ, et al. Mutations of the forkhead/winged-helix gene, *FKHL7*, in patients with Axenfeld-Rieger anomaly. Am. J. Hum. Genet 1998;63:1316–1328. [PubMed: 9792859]
28. Gould DB, Mears AJ, Pearce WG, Walter MA. Autosomal dominant Axenfeld-Rieger anomaly maps to 6p25. Am. J. Hum. Genet 1997;61:765–768. [PubMed: 9326342]
29. Nishimura DY, et al. The forkhead transcription factor gene *FKHL7* is responsible for glaucoma phenotypes which map to 6p25. Nat. Genet 1998;19:140–147. [PubMed: 9620769]

30. Saleem RA, Banerjee-Basu S, Berry FB, Baxevanis AD, Walter MA. Analyses of the effects that disease-causing missense mutations have on the structure and function of the winged-helix protein FOXC1. Am. J. Hum. Genet 2001;68:627–641. [PubMed: 11179011]

31. Lehmann OJ, Sowden JC, Carlsson P, Jordan T, Bhattacharya SS. Fox's in development, disease. Trends Genet 2003;19:339–344. [PubMed: 12801727]

32. Ormestad M, Astorga J, Carlsson P. Differences in the embryonic expression patterns of mouse Foxf1 and −2 match their distinct mutant phenotypes. Dev. Dyn 2004;229:328–333. [PubMed: 14745957]

33. Hong HK, et al. The winged helix/forkhead transcription factor Foxq1 regulates differentiation of hair in satin mice. Genesis 2001;29:163–171. [PubMed: 11309849]

34. Hayashi H, Kume T. Foxc transcription factors directly regulate Dll4 and Hey2 expression by interacting with the VEGF-Notch signaling pathways in endothelial cells. PLoS One 2008;3:e2401. [PubMed: 18545664]

35. Philip N, et al. Mutations in the oligophrenin-1 gene (*OPHN1*) cause X linked congenital cerebellar hypoplasia. J. Med. Genet 2003;40:441–446. [PubMed: 12807966]

36. Najm J, et al. Mutations of *CASK* cause an X-linked brain malformation phenotype with microcephaly and hypoplasia of the brainstem and cerebellum. Nat. Genet 2008;40:1065–1067. [PubMed: 19165920]

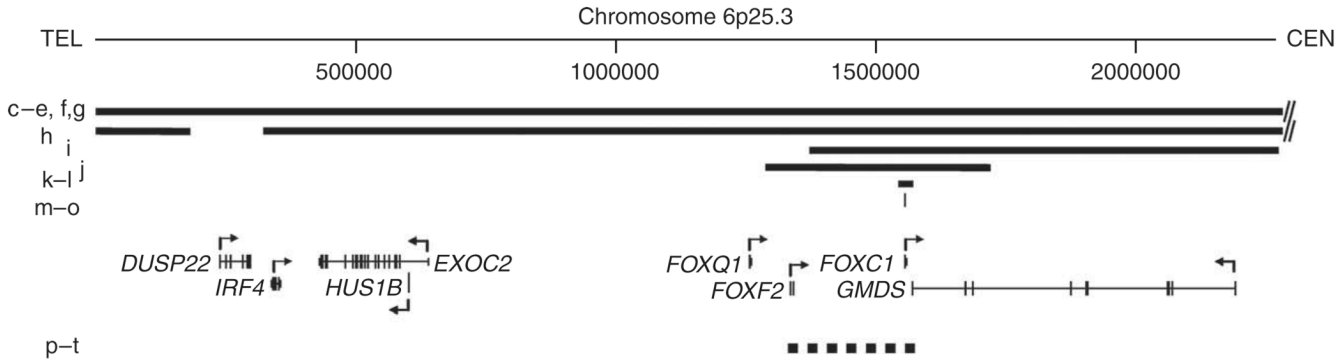

Figure 1.

Physical map of the 6p25.3 DWM locus. Diagram of 6p25.3 drawn to scale shows deletions (solid bars) and duplications (dashed bar) as well as heterozygous mutations of *FOXC1* (thin vertical line). Letters to the left of the CNVs refer to the same patients as in Figure 2. RefSeq genes are shown with direction of transcription (arrows). Chromosome position is given in kb.

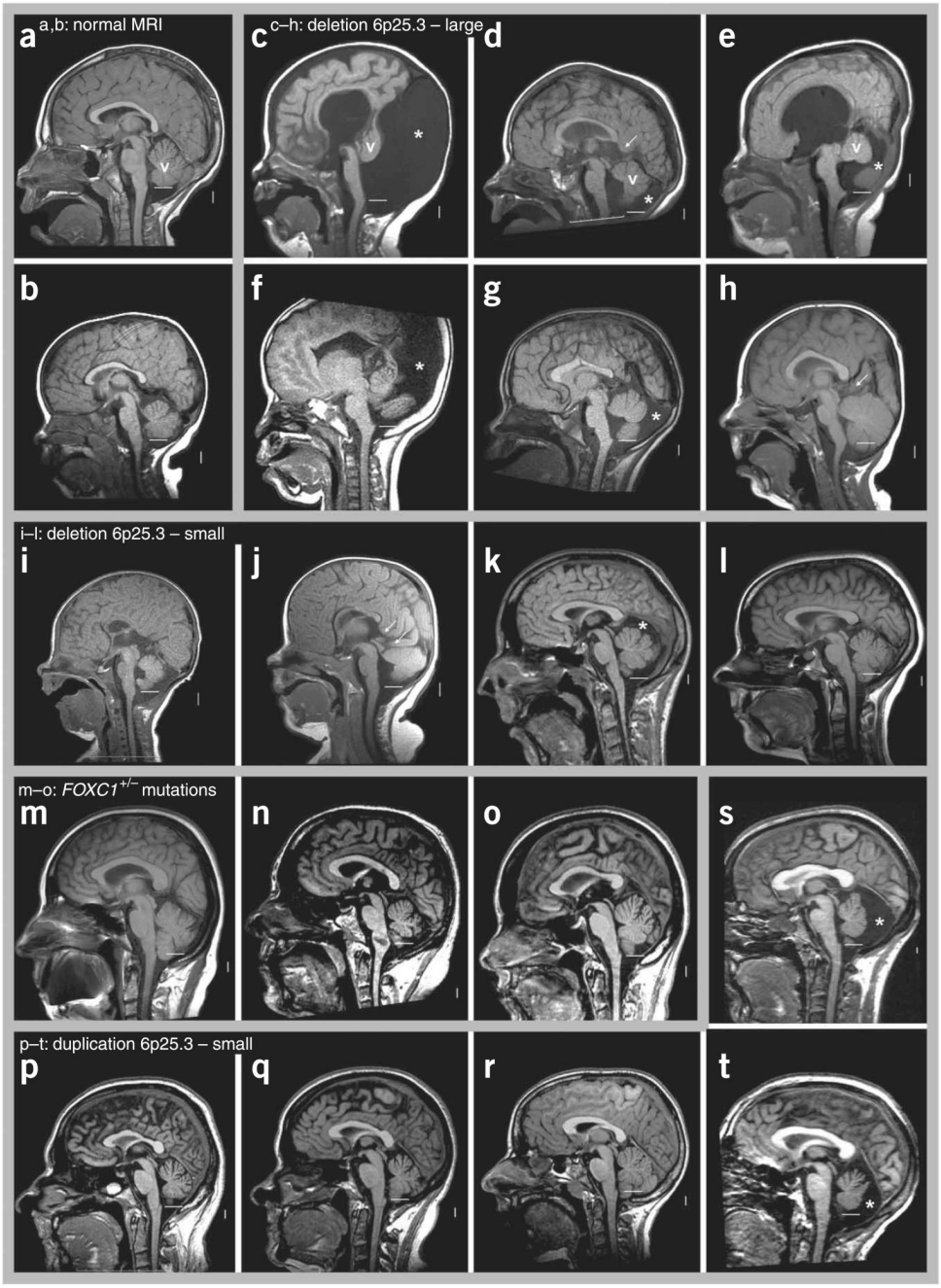

Figure 2.

Brain images of affected individuals within the 6p25.3 cohort. (**a–t**) T_1-weighted midsagittal magnetic resonance images in two control subjects (**a,b**) and 18 subjects with 6p25.3 CNVs that include *FOXC1* or intragenic mutations of *FOXC1* (**c–t**). The midline cerebellar vermis (v) is marked only in the top row of images. The lower limit of the vermis typically extends down to the obex, marked by a horizontal white line in each image. In all but one individual (**h**), the lower border of the vermis does not reach the white line, indicative of cerebellar vermis hypoplasia (CVH). Asterisks (*) indicate an enlarged posterior fossa. In 5/6 individuals with large deletions of 6p25.3 (**c–g**), brain images show a small and upwardly rotated vermis, cystic dilatation of the fourth ventricle and an enlarged posterior fossa, meeting criteria for classic

Dandy-Walker malformation (DWM). The remaining individual (**h**) unexpectedly has a normal or mildly enlarged vermis. The vermis appears abnormal in all four individuals with small deletions of 6p25.3 (**i–l**). The first two (**i,j**) meet criteria for DWM, although the abnormalities are less severe than in the subject with larger deletions. The next (**k**) has mild CVH with normal vermis position (not rotated upward), a normal fourth ventricle and mildly enlarged posterior fossa, consistent with mega-cisterna magna (MCM). The last individual in this group (**l**) has mild CVH only. The three individuals with heterozygous intragenic *FOXC1* mutations (**m–o**) all have mild CVH only. Among the five individuals with 6p25.3 duplication, two sibs (**p,t**) have obvious MCM, whereas three other sibs—probably distantly related to the first two—have mild CVH only.

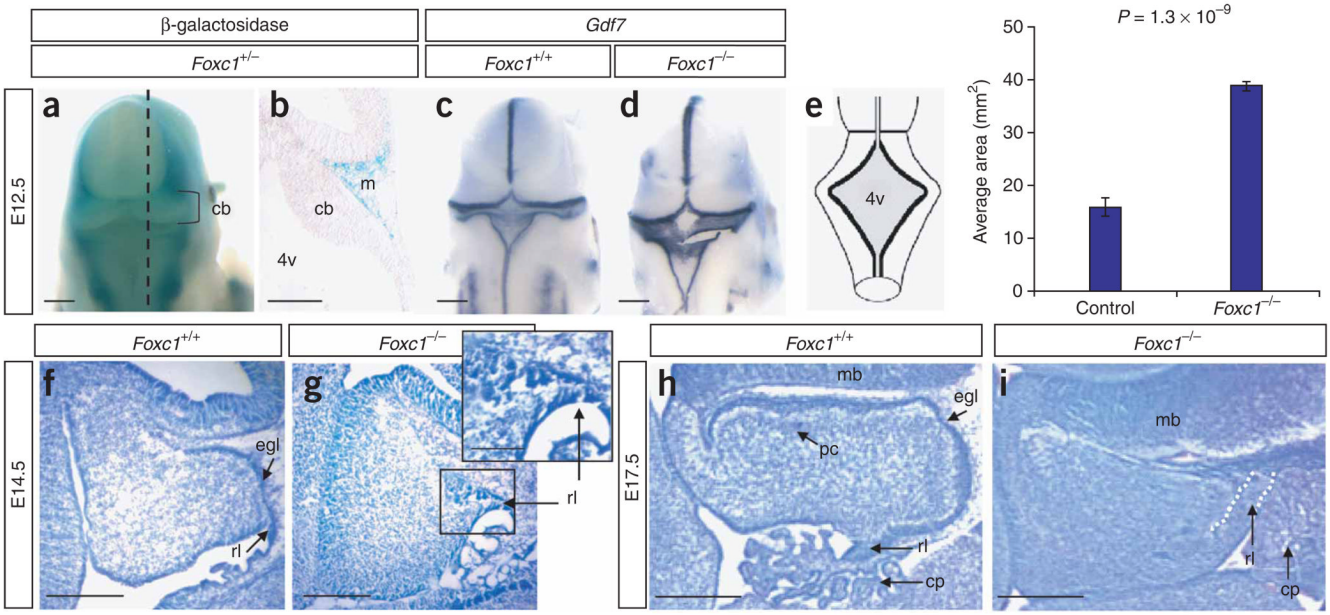

Figure 3.

Morphological cerebellar phenotype of *Foxc1* $^{-/-}$ embryos. (**a**) Dorsal view of the head from an X-gal–stained *Foxc1* $^{+/-}$ (*Mf1* $^{+/LacZ}$) embryo at E12.5 showing that *Foxc1* expression excludes the developing brain. (**b**) Midsagittal section through embryo in a (dashed line) showing expression in the mesenchyme (**m**) adjacent to the cerebellar anlage (cb). (**c**) Dorsal view of *Gdf7* expression in a wild-type embryo. (**d**) Dorsal view of *Gdf7* expression in a *Foxc1* $^{-/-}$ embryo revealing an enlarged fourth ventricle roof plate (4v). (**e**) Schematic of the dorsal view of an E12.5 embryo depicting the 4v area (shaded gray) measured in *Foxc1* $^{-/-}$ and littermates. The 4v was 2.5-fold larger in *Foxc1* $^{-/-}$ embryos. (**f**) Cresyl violet–stained midsagittal section of the developing cerebellar anlage in a wild-type E14.5 embryo. (**g**) Midsagittal section of the developing cerebellar anlage in a *Foxc1* $^{-/-}$ E14.5 embryo showing that the rhombic lip (rl) and external granule cell layer (egl) are abnormal and highly disorganized. (**h**) Midsagittal section through the cerebellar vermis of a wild-type E17.5 embryo showing distinct egl and Purkinje cell (pc) layers. (**i**) Midsagittal section through the cerebellar vermis of a *Foxc1* $^{-/-}$ E17.5 embryo showing a lack of distinct egl and pc layers, an abnormal rl and an expansion of the choroid plexus (cp). Scale bars, 100 (**a,c,d**), 50 (**b,f–i**) or 20 μm (**g** inset).

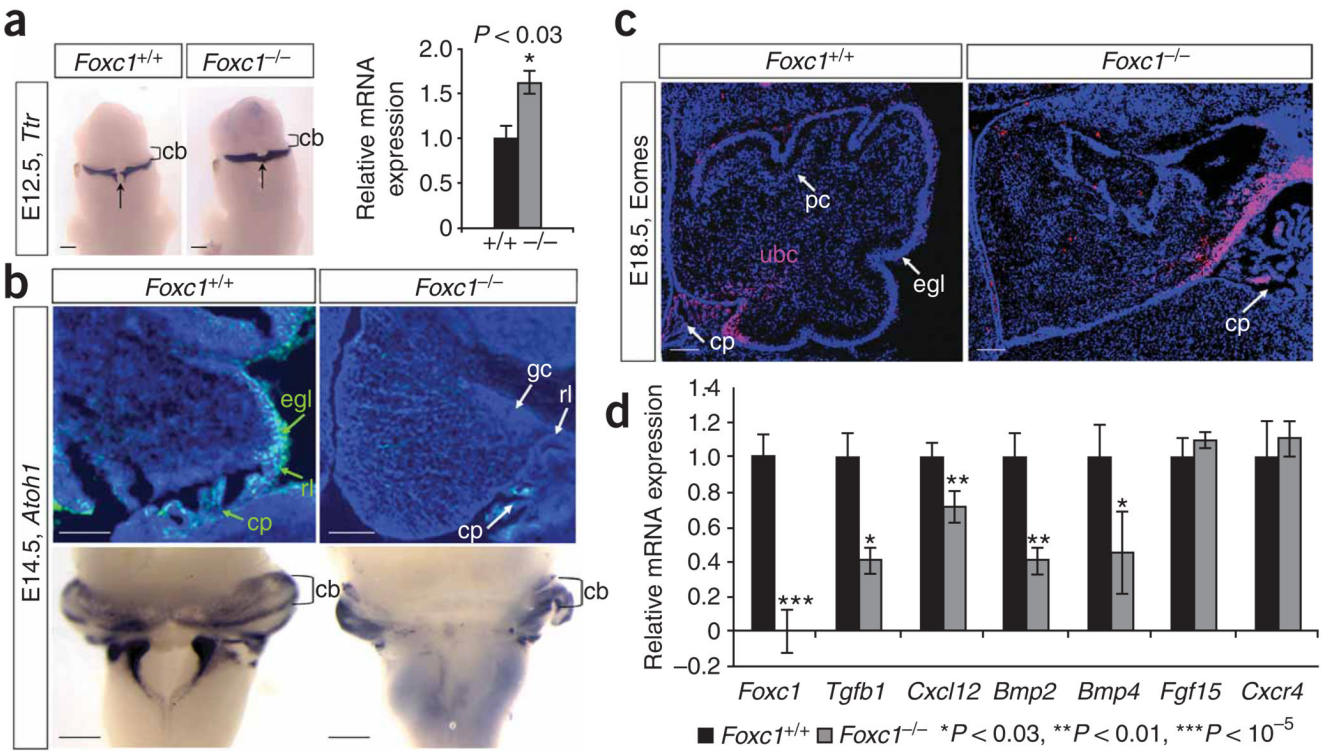

Figure 4.

Loss of *Foxc1* from hindbrain mesenchyme disrupts rhombic lip–derived cerebellar cellular populations. (**a**) *Ttr* expression in the differentiating choroid plexus epithelium of E12.5 WT and *Foxc1* $^{-/-}$ littermate embryos assayed by *in situ* hybridization (ISH) shows midline expansion of choroid plexus (arrow) adjacent to the cerebellar anlage (cb) in the mutant. Increased *Ttr* expression confirmed by qRT-PCR (relative to *Gapdh* expression) is presented as mean ± s.e.m. **P* < 0.03 (**b**) DAPI-counterstained (blue) parasagittal section shows Atoh1 expression (green) in the cerebellar anlage of E14.5 W Tand *Foxc1* $^{-/-}$ littermate embryos. No Atoh1^{+} cells are observed in the mutant egl. Whole-mount ISH of E14.5 brains confirms that loss of *Atoh1* in the mutant is restricted to the developing cerebellar vermis. (**c**) Eomes expression (pink) in the cerebellar anlage of E18.5 WT and *Foxc1* $^{-/-}$ littermate embryos. The Eomes^{+} unipolar brush cells (ubc) remain in the rl of the mutant, rather than migrating through the developing white matter as in WT. DAPI staining (blue) shows egl and pc in WT cerebellum. (**d**) Expression of six known *Foxc1* downstream targets in eye mesenchyme and endothelial development in the mid-hindbrain of E12.5 WT (black) and *Foxc*1$^{-/-}$ (gray) littermate embryos, assayed by qRT-PCR. Loss of *Foxc1* significantly decreases expression of genes secreted from hindbrain mesenchyme (*Tgfb1*, *Cxcl12*, *Bmp2* and *Bmp4*) but not genes expressed in the neural tube (*Fgf15* and *Cxcr4*). Data presented as mean ± s.e.m. represent four independent experiments. **P* < 0.03, ***P* < 0.01, ****P*< 0.00001. Scale bars, 100 μm.

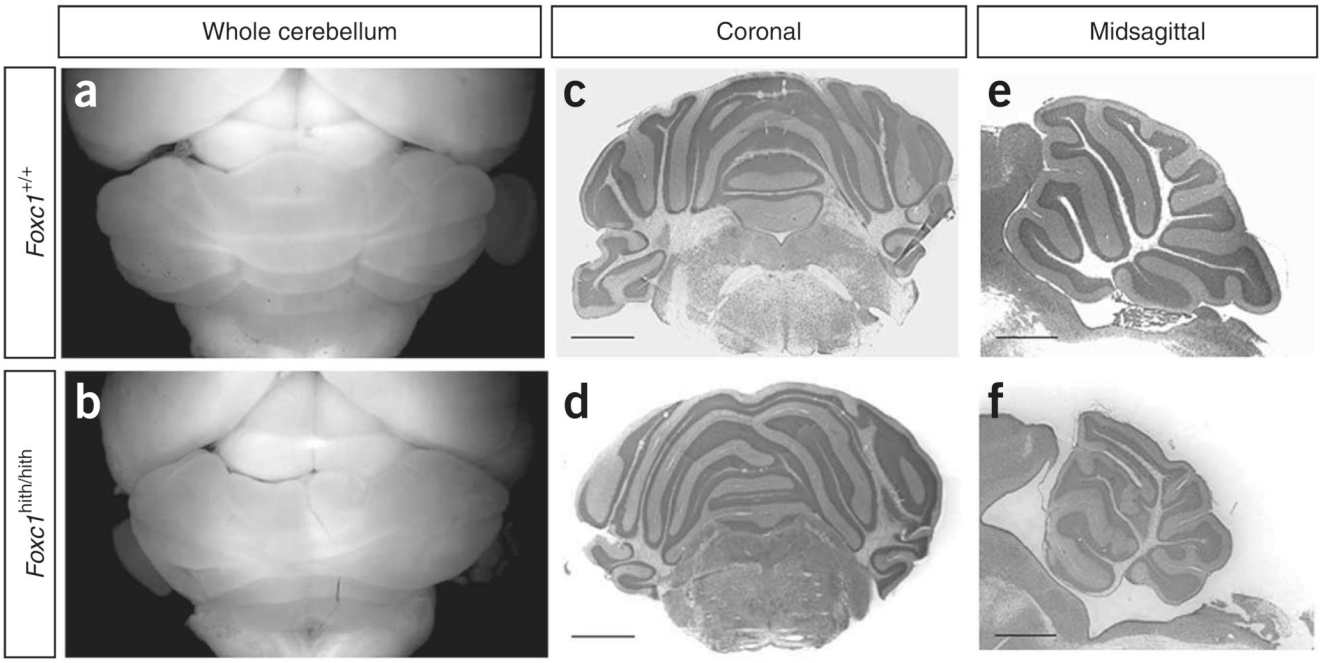

Figure 5.

Cerebellar morphology of *Foxc1* $^{hith/hith}$ mice. (**a,b**) Dorsal views of mouse brains at postnatal day (P) 30. Mean cerebellar area between *Foxc1* $^{hith/hith}$ (5.63 arbitrary units (a.u.) ± 0.31 s.e.m.) and littermates (8.60 a.u. ± 0.03 s.e.m.) reveals significant hypoplasia in these adult mutants ($P < 0.01$). (**c,d**) Cresyl violet–stained coronal sections through the cerebellum. (**e,f**) Cresyl violet–stained midsagittal sections through the vermis of brains of mice at P30. The wild-type cerebellum (**a**) has a stereotypic foliation pattern, which is disrupted in the homozygous mutants. Scale bars, 200 μm.

Nat Genet. Author manuscript; available in PMC 2010 September 1.

Table 1

Genotype-phenotype analysis of affected subjects with CNV of 6p25.3 or mutations of *FOXC1*

Subject	Inheritance	MRI[g]	Sex	CNV[h] (Mb)	Vermis size[j]	Vermis rot[k]	PF[l]	DX[m]	CC[n]	Men def[o]	WM[p]	Reference
Del 6p25.3												
LR04-301	*De novo*	2c	F	>5[i]	↓↓	↑↑	↑↑	DWM	−	−	−	Subject 1[7]
LR04-302	*De novo*	2d	F	>5[i]	↓	↑	↑	dwm	−	+	+	Subject 3[7]
LR04-303	Unknown[a]	2e	F	>5[i]	↓↓	↑↑	↑↑	DWM	−	−	−	Subject 2[7]
LR04-317	Unknown[b]	2f	F	4.95	↓↓	↑↑	↑↑	DWM	+	−	−	001-1[5]
LR04-313a2	Unknown[c]	2g	F	3.94	↓↓	↑↑	↑↑	DWM	−	+	+	002-2[5,6]
LR04-318a1	Familial[d]		F	3.94	↓↓	↑↑	↑↑	DWM	…	…	…	003-1[5]
LR04-318a2	Familial[d]		F	3.94	↓↓	↑↑	↑↑	DWM	…	…	…	003-2[5]
LR07-237	*De novo*	2h	M	1.9	−	−	↑	Text	−	+	−	Proband 11[9]
LR08-198	*De novo* [e]	2i	M	0.45	↓↓	↑	−	dwm	+	+	−	Subject[8]
LR07-072	*De novo*	2j	F	0.870	↓	↑	↑	dwm	+	++	−	Pedigree 10[9]
LR08-197a1	Familial[f]	2k	M	0.030	↓	−	↑	MCM	−	−	±	Pedigree 9[9]
LR08-197a2	Familial[f]	2l	F	0.030	↓		−	CVH	−	−	−	Pedigree 9[9]
FOXC1 [+/−]												
LR08-027a1	Familial	2m	F	p.S82T	↓	−	−	CVH	−	+	+	Family 3[27,28]
LR08-027a2	Familial	2n	M	p.S82T	↓	−	−	CVH	−	−	+	Family 3[27,28]
LR08-075	Familial	2o	F	p.S131L	↓	−	−	CVH	−	−	+	S131L[29]
Dup 6p25.3												
LR06-253a1	Familial	2p	U	0.492	↓	−	↑	MCM	…	…	…	Pedigree 5[9]
LR06-253a2	Familial	2t	U	0.492	↓	−	↑	MCM	…	…	…	Pedigree 5[9]
LR07-230a1	Familial		M	0.492	↓		−	CVH	−	−	++	Pedigree 6[9]
LR07-230a2	Familial	2q	M	0.492	↓	−	−	CVH	−	−	−	Pedigree 6[9]
LR07-230a3	Familial	2r	F	0.492	↓	−	−	CVH	−	−	−	Pedigree 6[9]

Subject	Inheritance	MRI[g]	Sex	CNV[h] (Mb)	Vermis size[j]	Vermis rot[k]	PF[l]	DX[m]	CC[n]	Men def[o]	WM[p]	Reference
LR07-230a4	Familial	2s	M	0.492	↓	−	−	CVH	−	−	−	Pedigree 6[9]

Phenotype data are grouped by mutation type.

[a] Mother normal, father not tested.

[b] Parents clinically normal, but chromosomes not tested.

[c] Affected sibling, but parents not tested.

[d] Maternal 6p;16q translocation.

[e] Unbalanced 6p;18p translocation.

[f] Postzygotic mosaicism in one parent.

[g] Indicates the panel in Figure 2 showing the subject's midline sagittal MRI.

[h] CNV, copy number variants (size listed in Mb) or *FOXC1* mutation, listed as the protein (amino acid) change.

[i] Large visible deletions of chromosome 6q25 by clinical karyotype analysis indicated as >5 Mb, although no molecular studies were performed.

[j] Cerebellar vermis size is graded as mild (↓) or moderate to severe (↓↓) hypoplasia.

[k] Upward rotation (rot) of the vermis is graded as mild (↑) or moderate to severe (↑↑).

[l] Posterior fossa (PF) enlargement is graded as mild (↑) or moderate to severe (↑↑).

[m] Brain imaging diagnosis (DX) is designated as typical (CVH) or mild (cvh) cerebellar vermis hypoplasia, classic (DWM) or mild (dwm) Dandy-Walker malformation, or mega-cisterna magna (MCM), which also includes mild hypoplasia of the posterior vermis. 'Text', see Supplementary Note for diagnosis.

[n] Corpus callosum (CC) size is graded as normal (−) or as short (+) consistent with mild partial agenesis.

[o] Meningeal defects (Men def) present as inappropriate interdigitation of right- and left-sided cerebral gyri secondary to deficiency of the falx cerebri, as medial and anterior displacement of medial parietal gyri into the potential space located between the splenium of the CC and cerebellar vermis secondary to deficiency of the tentorium cerebelli, or both.

[p] Abnormal white matter (WM) signal on T_2 or Flair sequences typically correspond to prominent perivascular spaces (+), although one aged subject had more severe changes (++).